

# Adeno-associated virus serotype 8 efficiently delivers genes to muscle and heart

Zhong Wang<sup>1,3</sup>, Tong Zhu<sup>1,3</sup>, Chunping Qiao<sup>1</sup>, Liqiao Zhou<sup>1</sup>, Bing Wang<sup>1</sup>, Jian Zhang<sup>1</sup>, Chunlian Chen<sup>1</sup>, Juan Li<sup>1</sup> & Xiao Xiao<sup>1,2</sup>

Systemic gene delivery into muscle has been a major challenge for muscular dystrophy gene therapy, with capillary blood vessels posing the principle barrier and limiting vector dissemination. Previous efforts to deliver genes into multiple muscles have relied on isolated vessel perfusion or pharmacological interventions to enforce broad vector distribution. We compared the efficiency of multiple adeno-associated virus (AAV) vectors after a single injection via intraperitoneal or intravenous routes without additional intervention. We show that AAV8 is the most efficient vector for crossing the blood vessel barrier to attain systemic gene transfer in both skeletal and cardiac muscles of mice and hamsters. Serotypes such as AAV1 and AAV6, which demonstrate robust infection in skeletal muscle cells, were less effective in crossing the blood vessel barrier. Gene expression persisted in muscle and heart, but diminished in tissues undergoing rapid cell division, such as neonatal liver. This technology should prove useful for muscle-directed systemic gene therapy.

Medicine currently offers no effective treatment for muscular dystrophies, which afflict a significant population of children and adults worldwide. Gene therapy has great potential for the treatment of genetic muscle diseases<sup>1–4</sup>. A major challenge is how to deliver the therapeutic genes into most, if not all, of the diseased muscles. Previously, muscle tissue has been targeted to produce therapeutic proteins for gene therapy of metabolic diseases<sup>5–7</sup>. Delivery of gene vectors to local muscle or heart tissue has been achieved by direct intramuscular (i.m.) injection<sup>8–11</sup> or by local blood vessel perfusion with both nonviral and viral vectors, including plasmid DNA<sup>12</sup>, adenovirus<sup>13</sup> and adeno-associated (AAV) vectors<sup>13–15</sup>. Long-term therapy of diseased muscles has been achieved with numerous treatments, particularly with AAV vectors<sup>1,2,4,7,15–18</sup>. However, multiple intramuscular injections of the gene vector remain impractical for large groups of muscles. Currently available techniques for blood vessel-mediated gene delivery in muscle (isolated limb perfusion) require the assistance of either pharmacological reagents to enhance vasculature permeability<sup>13</sup> or physical interference, such as large-volume and high-pressure injection, to force the vector particles out of the blood vessels and into the muscle tissues<sup>12</sup>. As a result, these methods are not feasible for whole-body vector delivery.

We have focused on AAV vectors because of their effectiveness for systemic muscle gene delivery<sup>8–11,19</sup>. In addition to the advantages of nonpathogenicity, robust infectivity and long-term gene transfer in both skeletal and cardiac muscles, AAV is the smallest virus that has been widely used as a gene vector system. With a diameter of ~20 nm, the physical particles of AAV are even smaller than naked plasmid DNA<sup>20,21</sup> and other viral and nonviral vectors such as adenovirus, lenti- and retrovirus, herpes simplex virus and liposomes, which have

diameters of ~100 nm or larger. Even though smaller particles have intrinsic advantages in crossing the physical barriers of both the blood vessels and basal lamina of differentiated muscle cells<sup>22</sup>, our attempts to deliver AAV serotype-2 vectors into multiple muscles have been unsuccessful. This suggests that it is just as important to overcome biological as physical barriers in achieving efficient vector dissemination and infection of muscle tissues.

Recently, a number of new AAV serotype vectors, including AAV7 and AAV8, have become available<sup>23–25</sup> and have made it possible to reexamine the feasibility of systemic muscle gene delivery. Because different AAV vectors exhibit distinct tissue tropism and interact with different cellular receptors<sup>26–29</sup>, we investigated the behavior of the new serotype vectors with regard to systemic delivery. Using intraperitoneal or intravenous vector delivery methods in neonatal and adult mice and hamsters, we observed profound differences in systemic vector dissemination and transgene expression in striated muscles by different AAV serotype vectors. Whereas AAV8 showed the highest efficiency in systemic gene transfer to striated muscles throughout the whole body, AAV1 and AAV6 were the most efficient in local muscle gene delivery by direct intramuscular injection.

## RESULTS

### Diverse efficiencies in systemic muscle gene transfer with AAV vectors

Our initial intention was to target the respiratory muscles, such as diaphragm and abdominal muscles, by injecting AAV vectors into the peritoneal cavity of neonatal mice. Based on previous experience in muscle tissues<sup>19,24</sup>, we chose to compare AAV serotypes 1, 2, 5, 6, 7 and 8. Each of these AAV vectors contained an identical vector DNA

<sup>1</sup>Dept. of Molecular Genetics and Biochemistry, and <sup>2</sup>Dept. of Orthopedic Surgery, University of Pittsburgh School of Medicine, 200 Lothrop Street, Pittsburgh, Pennsylvania 15261, USA. <sup>3</sup>These two authors contributed equally to this work. Correspondence should be addressed to X.X. ([xiaox@pitt.edu](mailto:xiaox@pitt.edu)).

Published online 27 February 2005; doi:10.1038/nbt1073

cassette that harbors a gene encoding green fluorescent protein (GFP) driven by a constitutive CB promoter<sup>30,31</sup>. We could directly monitor and compare both short- and long-term transgene expression in a variety of organs and tissues. As expected, we observed a wide range of gene transfer efficiencies 2 months after intraperitoneal (i.p.) injection of different AAV vectors in neonatal mice (**Fig. 1a**). Whole-body fluorescent photography revealed strong and widespread GFP expression in chest and hind leg muscles from both ventral and dorsal views after AAV1, 6, 7 and 8 vector treatment (**Fig. 1a**), and more widespread expression in the forelimb and shoulder muscles after AAV7 and 8 treatment. Lower levels of fluorescence were observed in the AAV5- and AAV2-treated mice, mainly in the abdominal muscle and localized on the vector injection side (**Fig. 1a**). GFP expression started as early as 3 d after i.p. injection of AAV8 vectors and gradually increased and persisted to adulthood in the vast majority of the muscles throughout the body (**Fig. 1b**). These results indicate that AAV1, 6, 7 and most particularly AAV8 are highly efficient in transducing muscles beyond the intraperitoneal cavity.

We next examined GFP transgene expression semi-quantitatively with fluorescent microscopy on muscle cross-sections, because whole-body fluorescence photography had low sensitivity and low depth of detection. AAV8 vector-treated mice again exhibited strong GFP expression in all the skeletal muscles examined (**Fig. 1c** and data not shown). Highly efficient transduction was also observed in cardiac muscle (**Fig. 1c**). Comparison of GFP expression by various AAV serotype vectors revealed that AAV7 and particularly AAV8 effectively transduced muscles not only in the vicinity of the peritoneal cavity and hind limbs, but also at remote sites such as forelimb, facial and

heart muscles (**Fig. 1d**). These results suggest that AAV8 is the most effective serotype in transducing the vast majority of striated muscles. Because AAV7 had a similar, but slightly weaker, profile than AAV8, we elected not to characterize both viruses in parallel in the subsequent experiments.

AAV1, 5 and 6 vectors were less effective than AAV7 and AAV8 in transducing remote muscle sites. Although AAV1 and 6, the two serologically identical vectors<sup>25</sup>, yielded the strongest GFP expression in many muscles, they also showed a high degree of preference for the abdominal wall, chest wall and hind limbs, as revealed by both whole-body fluorescence photography (**Fig. 1a**) and semi-quantitative fluorescent microscopy of muscle cryosections (**Fig. 1d**). A gradient of fluorescence was often observed with prominent GFP expression on the left side of the body, where the vectors were initially delivered into the peritoneal cavity (**Fig. 1a**). Much weaker signals were detected in the forelimb and facial muscles of AAV1- and AAV6-treated mice, and background levels in AAV5-treated mice (**Fig. 1d**). Furthermore, AAV1 and 6 were substantially less efficient in transducing cardiac muscle when compared to AAV7 and 8, but much better than AAV5 and 2 (**Fig. 1d**).

We also examined nonmuscle tissues. In striking contrast to the broad and robust GFP expression in skeletal and cardiac muscle, GFP-positive cells were essentially undetectable in brain, spleen, gonad glands (testes and ovary), or smooth muscle of the intestine and blood vessels (data not shown) 2 months after vector delivery into neonatal mice with all six serotypes. Only a few sporadic positive green cells were detected in the lungs and kidneys of some mice (**Fig. 1c**). Less than 1% of the hepatocytes remained GFP-positive in the liver even after AAV8 treatment (**Fig. 1c**), which was

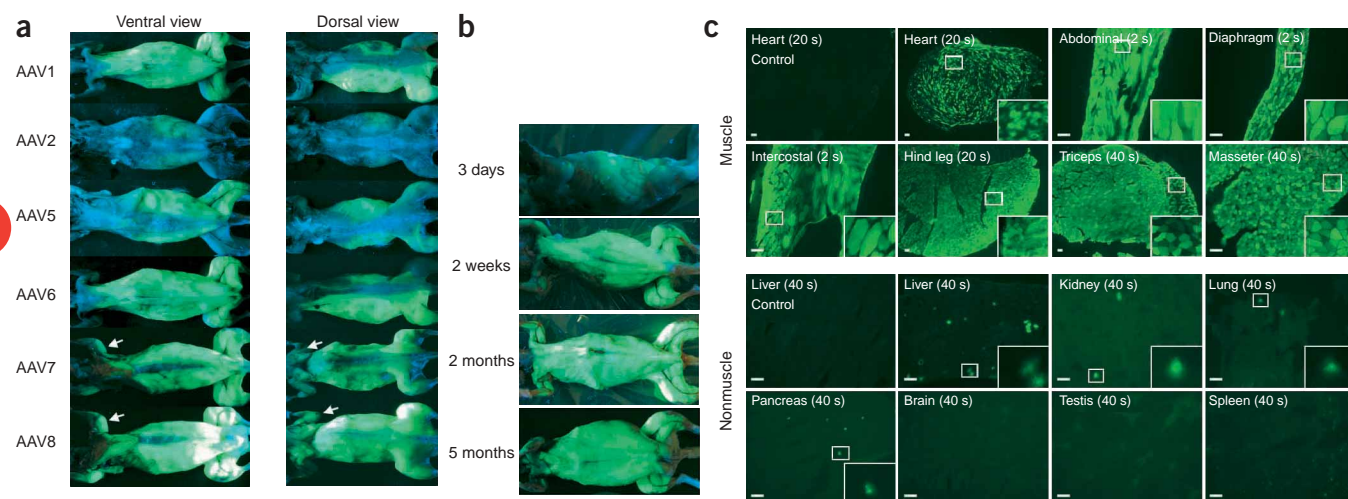


**Figure 1** Systemic gene delivery to muscle and heart of neonatal mice by different AAV serotypes via i.p. injection. **(a)** Whole-body fluorescent photography of 2-month-old mice after i.p. injection of  $2 \times 10^{11}$  v.g. of various dsAAV-CB-GFP at 1 d old. Note the widespread GFP expression in the foreleg, back and shoulder muscles in mice treated with AAV7 and AAV8. **(b)** Time course of GFP gene expression in mice after i.p. injection of  $2 \times 10^{11}$  v.g. of dsAAV8-CB-GFP at 6 d old. **(c)** GFP expression seen in cryosections of heart, muscle and nonmuscle tissues at 2 months after neonatal i.p. injection of  $2 \times 10^{11}$  v.g. of dsAAV8-CB-GFP. Numbers in parentheses denote microscopy exposure time in seconds (s). Note strong GFP expression in heart and muscles, and minimal to undetectable GFP expression in nonmuscle tissues. Scale bar, 100  $\mu$ m. **(d)** Quantification of GFP fluorescence in muscle and heart cryosections of mice, which were injected i.p. with  $2 \times 10^{11}$  v.g. of various serotypes of dsAAV-CB-GFP vectors at neonatal age. Analysis was done 2 months after gene delivery.

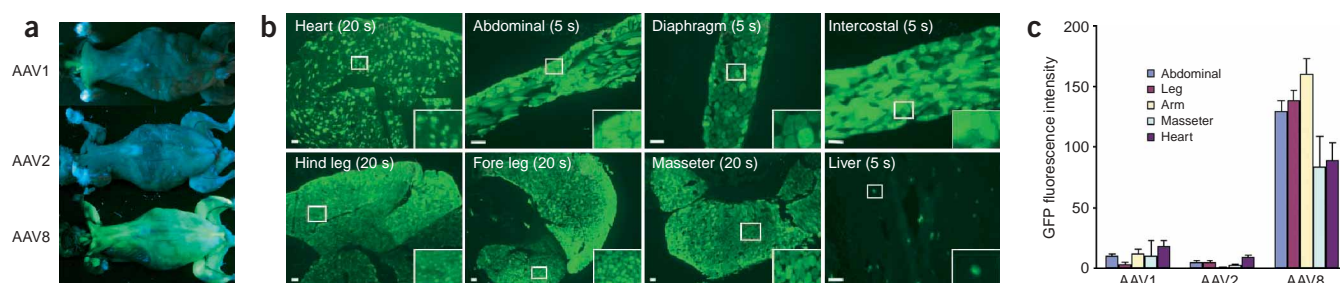


**Figure 2** Systemic gene delivery to muscle of neonatal mice by different AAV serotypes via i.v. injection. (a) Whole-body fluorescent photography taken one month after i.v. (temporal vein) injection of  $2 \times 10^{11}$  v.g. of various dsAAV-CB-GFP at 3 d of age. (b) GFP expression seen in cryosections of heart, muscle and nonmuscle tissues one month after neonatal i.v. injection with  $2 \times 10^{11}$  v.g. of dsAAV8-CB-GFP. Numbers in parentheses denote microscopy exposure time in seconds (s). Scale bar, 100  $\mu$ m. Note the strong GFP expression in heart and muscles, and the minimal to undetectable GFP expression in nonmuscle tissues. (c) Quantitative analysis of average fluorescence intensity of cryosections from various muscles of AAV1, 2 and 8 treated mice (as shown in a).

reportedly the most efficient vector for liver transduction<sup>24</sup>. This phenomenon is mainly due to vector instability in dividing cells and will be discussed later.

#### Intravenous administration of AAV8 vectors is most efficient for systemic muscle gene transfer in neonatal mice

Because i.p. vector delivery results preferentially in local muscle transduction, we next investigated intravenous (i.v.) delivery as an alternative approach. We compared AAV1, 2 and 8 by temporal vein injection in neonatal mice. As expected, AAV8 rendered the most efficient and persistent systemic transduction in both skeletal and cardiac muscles after i.v. injection (Fig. 2a), at the same vector dose ( $2 \times 10^{11}$  vector genome (v.g.)/mouse) and duration (2 months) as used in the i.p. studies (Fig. 1a and 1b). Importantly, i.v. injection yielded more balanced and uniform GFP expression in various muscle tissues (Fig. 2b). The average intensities of green fluorescence in facial, forelimb, hind limb and abdominal muscles were comparable (Fig. 2c). On the contrary, i.v. delivery of AAV1 and AAV2 vectors in neonatal mice resulted in much less efficient systemic transduction (Fig. 2a,c). These results strongly suggest that blood vessel-mediated dissemination is a major route for systemic muscle gene transfer after both i.v. and i.p. injections of AAV8, but not for AAV1 or 2. GFP expression in nonmuscle tissues such as the liver (Fig. 2b) was not persistent after i.v. administration, similar to i.p. injection.

#### Systemic gene transfer intravenously in adult mice and hamsters

We next investigated whether intravenous injection of AAV8 vectors in adult mice could also achieve systemic gene delivery to muscle and heart. Two-month-old mice were injected with the AAV8 vector via the tail vein at a dose of  $2 \times 10^{12}$  v.g. ( $6 \times 10^{10}$  v.g./g body weight)—close to the dose used in neonates on the basis of body weight ( $1 \times 10^{11}$  v.g./g body weight). One month after i.v. injection, adult mice also showed strong GFP expression in the heart and to a lesser degree in various skeletal muscles (Fig. 3a). The GFP expression in muscle was not strong enough to be detected by whole-body fluorescent photography (data not shown), suggesting that systemic vector delivery in adult mice is achievable, but less efficient than in neonates. Intravenous injection of other AAV serotype vectors including AAV1, 2, 5 and 6 at the same dose, however, resulted in much lower GFP expression in muscle and heart (data not shown).

A notable difference between adult and neonatal delivery of AAV8 was the persistent GFP gene expression in adult nonmuscle

tissues, particularly the liver, followed by the pancreas and gonads (Fig. 3a). The interstitial cells of the gonads showed significant GFP expression (Supplementary Fig. 1a online), but the copy number of the AAV vector DNA in the gonads was very low on the per diploid cellular genome basis, as shown by quantitative PCR analysis (Supplementary Fig. 1b online). This was expected and might be due to the lower number of interstitial cells among the highly packed spermatocytes. However, the lung, spleen and brain displayed very low or undetectable levels of GFP expression in both adult and neonatally treated mice.

We next compared the systemic gene transfer efficiency of AAV1, 6 and 8 in the presence or absence of a vasculature-permeable agent, vascular endothelial growth factor (VEGF), which was described in a recent report as enhancing gene transfer efficiency of AAV6 in adult mice<sup>32</sup>. We chose to use adult male ICR-CD1 mice, which were injected via the tail vein with  $1 \times 10^{12}$  v.g. of either AAV1, AAV6 or AAV8 GFP vectors, with or without 10  $\mu$ g VEGF<sup>32</sup>. The vectors were driven by the cytomegalovirus (CMV) promoter to attain strong cardiac expression. Two weeks after vector injection, however, no significant increase in GFP expression was observed in either skeletal or cardiac muscles under these conditions (Fig. 3b). However, in the pancreas and testis, an increase in GFP expression was observed in AAV1- and AAV6-treated mice after VEGF treatment (data not shown). The behavior of AAV8 was essentially unaffected by VEGF treatment.

To confirm the gene transfer efficiency in a different species, we examined AAV8-mediated systemic delivery in hamsters. Adult male F1B hamsters (6 weeks old, 60–70 g) were injected via the jugular vein with  $8 \times 10^{11}$  v.g. ( $1.3 \times 10^{10}$  v.g./gram of body weight) of either AAV2 or AAV8 vectors expressing GFP. Four months after vector injection, AAV8 vector-treated hamsters showed very strong GFP expression that could be readily detected by whole-body fluorescent photography (Supplementary Fig. 2 online). GFP expression in adult mice treated with AAV8 was insufficient to be detected by this method. Fluorescent microscopy on cryosections of hamster heart and various muscles confirmed the strong GFP gene expression after AAV8 vector treatment (Supplementary Fig. 2 online). As expected, AAV2 vector-treated hamsters showed minimal GFP expression in the heart and muscle (Supplementary Fig. 2 online).

In addition to the GFP reporter gene, we also tested a therapeutic gene delivered by the AAV8 vector, the  $\delta$ -sarcoglycan ( $\delta$ -SG) gene,



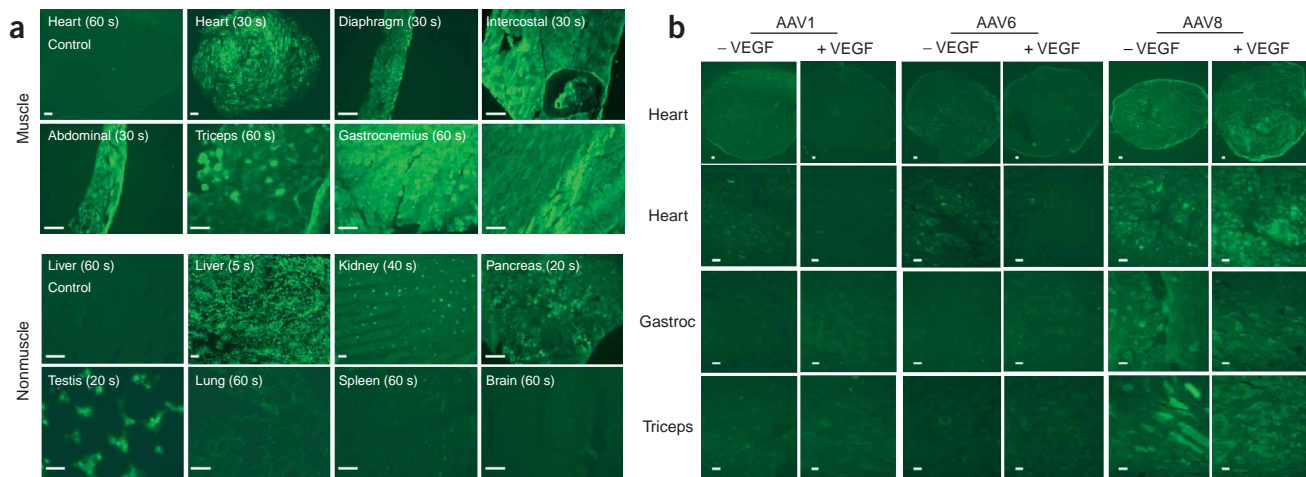


**Figure 3** Systemic gene delivery to muscle and heart by intravenous (i.v.) injection in adult mice and hamsters. **(a)** Fluorescent microscopy of cryosections of heart, muscle, and nonmuscle tissues for GFP expression one month after tail vein injection of  $2 \times 10^{12}$  v.g. of dsAAV8-CB-GFP in 10-week-old adult mice. Note that strong GFP expression is also seen in certain nonmuscle tissues such as liver, pancreas and testes, but undetectable in lung, spleen and brain. Numbers in parentheses denote microscopy exposure time in seconds (s). Scale bar, 100  $\mu$ m. **(b)** Comparison of AAV1, 6 and 8 for systemic muscle gene delivery in 2-month-old adult male mice with or without VEGF. Mice were injected via the tail vein with  $1 \times 10^{12}$  v.g. of dsAAV-CMV- GFP vectors, and sacrificed at 2 weeks after vector injection for muscle analysis. Fluorescence microscopy (60-s exposure) of cryosections of heart and muscles were taken. Scale bar, 100  $\mu$ m. **(c)** Dose escalation of dsAAV8- $\delta$ -SG vectors by i.p. injection in 10-day-old TO-2 hamsters led to lower and normal levels of muscle creatine kinase activities in sera. Shown were results at 4 months after gene delivery. WT, wild-type hamster F1B.

whose mutation causes limb girdle muscular dystrophy 2F and heart failure in the hamster model TO-2. Previously, we showed that local intramuscular injection of an AAV2- $\delta$ -SG vector in adult hamster legs could effectively alleviate the pathological signs of the dystrophic muscle<sup>33</sup>. In this study, 6-week-old male TO-2 hamsters were systemically injected via the jugular vein  $1 \times 10^{12}$  v.g. with a AAV8- $\delta$ -SG vector driven by a muscle-specific promoter<sup>34</sup>. Analysis of heart and leg muscle at 7 months after vector delivery showed robust  $\delta$ -SG gene expression and correction of pathological signs of the dystrophic muscles, such as fibrosis, calcification, degeneration and regeneration (Supplementary Fig. 3 online). The serum level of muscle-specific creatine kinase (CK) was also normalized in those hamsters (data not shown). Overexpression of  $\delta$ -SG was observed in the heart muscle, where many cardiomyocytes showed membrane as well as cytoplasmic staining of the  $\delta$ -SG<sup>13–15</sup>.

Finally, we carried out a vector dose-escalation experiment in 10-day-old TO-2 hamsters (about 10 g in weight) by intraperitoneal injection of different doses of the AAV8- $\delta$ -SG vector ranging from  $10^9$ – $10^{12}$  v.g. per animal. Because the untreated TO-2 hamster muscle cells were so leaky that their CK activities in the sera were 100–200 times higher than the normal hamster F1B, we used serum level measurements of muscle-specific creatine kinase (CK) as an indirect indicator of  $\delta$ -SG gene expression. Correction of CK leakage is an excellent indicator of the efficiency of whole-body therapeutic gene transfer. Data obtained 4 months after gene delivery showed a robust dose response (Fig. 3c). Higher vector doses ( $10^{11}$ – $10^{12}$  v.g./hamster) decreased serum CK levels by 200-fold, returning levels to baseline. These results indicated that the vast majority of the myofibers were biochemically corrected on the cell membrane due to systemic  $\delta$ -SG gene transfer and expression.

### AAV8 vectors effectively cross blood vessel barriers in muscle

Next, we investigated whether AAV8 vectors were more efficient in infecting muscle or in crossing the blood vessel barrier than other AAV serotypes. We first compared the capacity of AAV1, 2 and 8 in infecting muscle by direct intramuscular injection, hence bypassing the blood vessel barrier. Two months after an injection of  $1 \times 10^{10}$  v.g. in both hind leg muscles of neonatal mice, whole-body fluorescent photography showed that AAV1 vectors were superior to both AAV2 and AAV8 vectors in directly infecting muscle tissue. GFP expression by AAV1 was observed not only in both hind legs, but also in the abdominal and intercostal muscles (Fig. 4a). These results were similar to those obtained by i.p. injection of AAV1 in neonates (Fig. 1a). Similar profiles were obtained in adult mice after local i.m. injection in their hind legs (Fig. 4b). Interestingly, significant GFP expression was also observed in the heart after hind leg injection of AAV8, but not of AAV1 and AAV2 (data not shown). Such a phenomenon indicates stronger tropism of AAV8 vectors for heart muscle and effective dissemination through the blood stream.

We next tested the efficiency of AAV8 vectors in crossing the blood vessel barrier in muscle tissues. To avoid the interference of other organs such as the liver, we used the isolated hind limb perfusion method in adult mice. Identical doses of the AAV2 or AAV8 vectors were slowly perfused into the femoral vein without any other interventions such as high pressure/large volume, histamine or VEGF. As expected, strong and widespread GFP expression was readily visualized in the AAV8-perfused, but not the AAV2-perfused hind legs (Fig. 4c,d), and quantified (Fig. 4e). Consistent results were also obtained in hamsters using the same limb perfusion method with the AAV2 and AAV8 vectors (data not shown). These experiments support

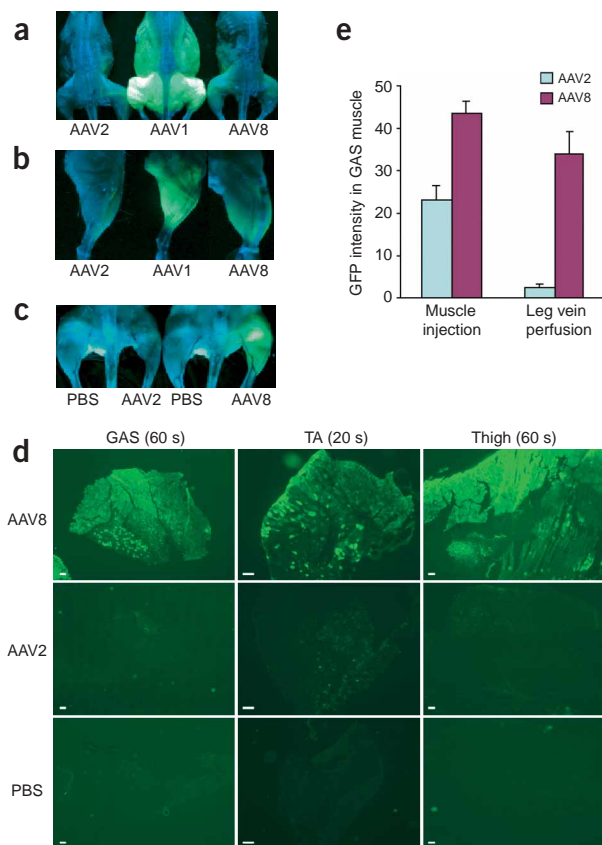


**Figure 4** Comparison of gene transfer efficiency of AAV serotype vectors by direct i.m. or i.v. injection on hind limbs. **(a)** Whole-body fluorescent photography shown at 1 month after i.m. injection of  $1 \times 10^{10}$  v.g. of various dsAAV-CB-GFP in the right and left hind legs of 1-week-old neonatal mice. **(b)** Fluorescent photography of hind legs shown at 1 month after i.m. injection of  $4 \times 10^{10}$  v.g. of dsAAV-CB-GFP in 2-month-old adult mice. **(c)** GFP expressions at 1 month after slow and retrograde perfusion of  $2 \times 10^{11}$  v.g. dsAAV-CB-GFP via the femoral vein of the hind leg of 8-week-old adult mice, of which the blood circulation in the hind leg was temporarily blocked during the procedure. **(d)** Fluorescent microscopy of cryosections of the hind leg muscles shown in **c**. Shown are the entire cross-sections of gastrocnemius (GAS), tibialis anterior (TA) and thigh muscles. Numbers in parentheses denote microscopy exposure time in seconds (s). Scale bar, 200  $\mu$ m. **(e)** Quantification of GFP fluorescence intensity in cryosections of gastrocnemius muscles of directly injected (as shown in **b**) and perfused (as shown in **c**) hind limbs.

growth, we performed Southern blot analysis of mouse liver DNA at different time points after AAV8 injection. DNA from the heart, which had stable GFP expression, was used as a control. High copy numbers of AAV8 genomes ( $> 50$  copies per cell) were detected in the liver at 3 d after injection (**Fig. 5b**). The majority of vector DNA existed as episomal supercoiled and linear monomers. The episomal AAV8 genomes rapidly decayed from more than 50 copies/cell on day 3 to less than 1 copy/cell by 2 months (**Fig. 5b**). By contrast, the vector copy number in the heart was much more stable. Most of the input linear monomer vector DNA was rapidly converted to circular monomers (**Fig. 5b**). Southern analysis of a wide range of tissues at 2 months after AAV8 i.p. injection also showed persistence of vector DNA in various skeletal muscles and in the heart (**Fig. 5c** and **Table 1**), but not in nonmuscle tissues including the liver, kidney, lung, pancreas and gonads (**Fig. 5c** and **Table 1**). These findings are consistent with their low level or lack of GFP expression (**Fig. 1c**). These results suggest that the loss of GFP expression in the liver and other tissues is mainly due to the loss of vector DNA.

## DISCUSSION

We have overcome the physical and biological barrier imposed by the capillary blood vessels of the muscle tissue on systemic gene delivery in neonatal mice with a single-dose of i.p. or i.v. administration of AAV vectors. In particular, AAV8 vectors led to efficient, systemic and prolonged transduction of skeletal and cardiac muscles and persisted into adulthood. Similar results were obtained in adult mice, although the efficiency was lower than in neonatal mice. Intraperitoneal injections of AAV vectors in adult mice resulted in more localized gene transfer than in the neonates, particularly in the abdominal and diaphragm muscles (data not shown). Lower efficiency in adult mice suggests that there exist additional barriers to systemic gene delivery that are not present in neonates. In addition, we have further shown the effectiveness of the AAV8 vector in both adult and neonatal hamsters, using either the GFP reporter gene

the notion that AAV8 is highly effective in crossing the blood vessel barrier of muscle tissues.

### Persistence of vector DNA in muscle and heart correlates with transgene expression

We next investigated why persistent gene expression was seen in the skeletal and cardiac muscles, but not in the liver and other tissues after neonatal delivery of AAV8 vectors. Time course analysis of GFP expression in the liver revealed that the difference was not due to the lack of gene transfer to the liver, because 3 d after i.p. injection the entire liver showed very strong green fluorescence (**Fig. 5a**). However, GFP expression rapidly declined over time. By 2 weeks, green fluorescence could no longer be detected by gross liver photography. By 2 and 5 months after injection, GFP expression further declined and was detectable in less than 1–2% of hepatocytes. By contrast, GFP expression in the skeletal and cardiac muscles increased greatly from 3 d to 2 weeks, and was sustained for 5 months (**Fig. 5a** and **Fig. 2b**).

To determine whether the rapid decline of GFP expression in liver was due to promoter shut off or loss of vector DNA during liver

**Table 1** AAV vector DNA distribution 2 months after i.p. injection in neonatal mice

	Abdominal	Diaphragm	Intercostal	Triceps	Masseter	Heart	Liver	Lung	Kidney	Spleen	Testis
AAV1	11	6	2	<0.1	<0.1	<0.1	<0.1	<0.1	<0.1	<0.1	–
AAV2	6	3	0.4	<0.1	<0.1	<0.1	<0.1	<0.1	<0.1	<0.1	–
AAV8	8	10	6	4	2	4	0.8	0.6	0.3	<0.1	<0.1

AAV vector DNA copy numbers in various tissues were determined by Southern blot analysis at 2 months after neonatal injection of  $2 \times 10^{11}$  dsAAV8-CB-GFP vector. Total DNA (10  $\mu$ g) from each tissue was double digested with *Bam*HI and *Xho*I, which dropped an internal fragment from the vector genomes. Semi-quantitative densitometry scanning of the X-ray film was performed and copy numbers determined against known amount of plasmid DNA reference standards. Copy numbers  $> 1$  were rounded up to the nearest integer.

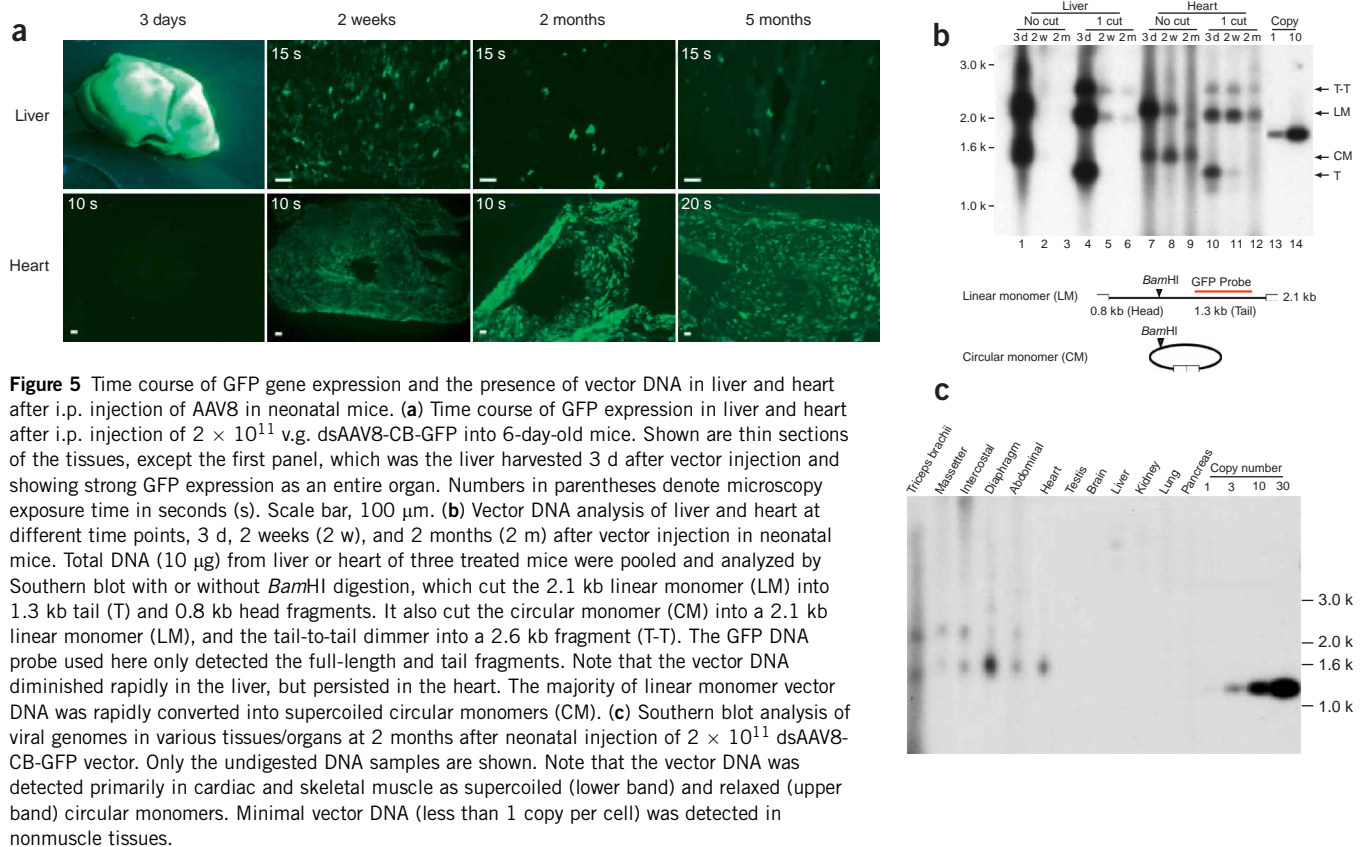


**Figure 5** Time course of GFP gene expression and the presence of vector DNA in liver and heart after i.p. injection of AAV8 in neonatal mice. **(a)** Time course of GFP expression in liver and heart after i.p. injection of  $2 \times 10^{11}$  v.g. dsAAV8-CB-GFP into 6-day-old mice. Shown are thin sections of the tissues, except the first panel, which was the liver harvested 3 d after vector injection and showing strong GFP expression as an entire organ. Numbers in parentheses denote microscopy exposure time in seconds (s). Scale bar, 100  $\mu$ m. **(b)** Vector DNA analysis of liver and heart at different time points, 3 d, 2 weeks (2 w), and 2 months (2 m) after vector injection in neonatal mice. Total DNA (10  $\mu$ g) from liver or heart of three treated mice were pooled and analyzed by Southern blot with or without *Bam*HI digestion, which cut the 2.1 kb linear monomer (LM) into 1.3 kb tail (T) and 0.8 kb head fragments. It also cut the circular monomer (CM) into a 2.1 kb linear monomer (LM), and the tail-to-tail dimer into a 2.6 kb fragment (T-T). The GFP DNA probe used here only detected the full-length and tail fragments. Note that the vector DNA diminished rapidly in the liver, but persisted in the heart. The majority of linear monomer vector DNA was rapidly converted into supercoiled circular monomers (CM). **(c)** Southern blot analysis of viral genomes in various tissues/organs at 2 months after neonatal injection of  $2 \times 10^{11}$  dsAAV8-CB-GFP vector. Only the undigested DNA samples are shown. Note that the vector DNA was detected primarily in cardiac and skeletal muscle as supercoiled (lower band) and relaxed (upper band) circular monomers. Minimal vector DNA (less than 1 copy per cell) was detected in nonmuscle tissues.

in normal hamsters or the  $\delta$ -sarcoglycan ( $\delta$ -SG) gene in muscular dystrophy hamsters.

The major difference between this and previous studies is the lack of additional interventions required for AAV8 vector transduction, such as the use of high pressure and large volume delivery<sup>12,35</sup> or the use of pharmaceutical reagents including histamine<sup>13,36</sup> and VEGF<sup>32</sup> for gene delivery in the limb<sup>12,13,35,36</sup>, heart<sup>14</sup> or the entire body<sup>32</sup>. We attribute the superiority of systemic gene delivery by AAV8 vectors to its capability to cross the blood vessel barrier. Our side-by-side comparison of AAV2 and AAV8 in direct intramuscular and intravascular injections in adult mouse and hamster hind limbs supports this notion. However, potential mechanisms such as transcytosis across the endothelial cells remain to be further investigated.

Recently, VEGF was used as a pharmaceutical reagent to increase blood vessel permeability and enhance whole-body gene delivery into muscle and heart tissues with AAV6 vectors<sup>32</sup>. However, these enhanced effects diminish at higher doses of AAV vectors<sup>32</sup> (also see Fig. 3b). Furthermore, the safety profile of high-dose VEGF administration and the secondary immune consequences such as the elevation of cytokines remain to be investigated<sup>37</sup>.

With systemic gene delivery comes unwanted gene transfer to other tissues such as the liver and gonads. This may pose safety concerns because of the potential to increase germline transmission. It is, therefore, highly desirable to achieve muscle-specific gene transfer and gene expression. An ideal vector system should demonstrate high efficiency at crossing the blood vessel barrier, high infectivity of muscle cells and minimal infectivity of nonmuscle cells. Such specificity could be achieved through multi-layer mechanisms: selection of naturally occurring viruses with high affinity to muscle tissues<sup>19</sup>, optimization

of viral tissue tropism by site-directed mutagenesis<sup>38</sup>, using chimeric viral particles consisting of a mixture of different serotype capsids<sup>39,40</sup>, modification of the viral particle surface with cell-specific ligands<sup>41–43</sup> and using muscle-specific promoters to limit gene expression in nonmuscle tissues.

Another mechanism observed in this study is the selective retention of vector DNA in muscle and heart cells after systemic gene delivery in neonatal mice. Despite the fact that AAV8 was highly effective at transducing cells in the liver, the vector DNA was rapidly degraded during liver growth and cell division. On the other hand, in tissues that undergo minimal cell division, such as heart and muscle, vector DNA persisted. However, this same phenomenon was not observed in adult mice because adult tissues, such as the liver, are largely quiescent, allowing vector DNA to remain stable. These findings suggest that systemic gene delivery in neonates may be a viable therapeutic option, particularly for childhood diseases with high mortality and morbidity that can be decreased with early intervention. Nonetheless, it remains a formidable challenge to translate the results from small rodents to large animals and eventually human patients.

## METHODS

**Vector production.** AAV vectors were generated by triple plasmid transfection of 293 cells<sup>44</sup>. For pseudo-typed AAV serotype vector production, the adenovirus helper plasmid XX6<sup>44</sup>, and the vector plasmid dsAAV-CB-GFP containing an GFP gene driven by the CB promoter<sup>30</sup>, or by CMV promoter were identical for all serotype vectors. Vector plasmid dsAAV8- $\delta$ -SG contains human  $\delta$ -sarcoglycan cDNA driven by the CMV promoter. The pseudo-typed AAV packaging plasmids, however, contained each individual serotype-specific capsid gene<sup>24,45,46</sup> and coupled with a universal AAV2 rep gene, which has



an ATG to ACG start codon mutation to increase the virus yield<sup>47</sup>. Thus, the resultant AAV serotype viral particles contained the identical AAV vector DNA cassette of GFP gene that was packaged by specific serotype capsids (AAV1, AAV2, AAV5, AAV6 and AAV7 and AAV8). Viruses were purified twice with CsCl gradient ultracentrifugation<sup>48</sup>. The titers of v.g. particles were determined by a standard dot-blot assay<sup>48</sup>.

**Animals and vector administration.** Housing and handling of the mice and hamsters are in compliance with the National Institutes of Health and institutional guidelines and approved by the Institutional Animal Care and Use Committee of the University of Pittsburgh. In detail, eight- to twelve-week adult mice and breeding pairs (ICR-CD1, C57BL10 mice) were purchased from Charles River and National Cancer Institute. Most of the experiments were done using the ICR-CD1 mice, which is an outbred strain. F1B and TO-2 males hamsters were purchased from Bio Breeders. For intra-peritoneal (i.p.) injection in neonatal mice, 100 µl of viral solution was slowly injected with a U-100 insulin syringe. For neonatal hamsters (10-day-old), 1 ml viral solution was used. For i.v. injections, temporal vein was used in neonates<sup>49</sup> and tail vein was used in adult mice. Intravenous vector administration in adult hamsters was performed via the jugular vein. For i.m. delivery in neonate mice, 30 µl of viral solution was injected into both left and right hind legs. For i.m. injection in adult mice, 50 µl of viral solution was directly injected into the gastrocnemius muscle.

Vector perfusion in mouse hind limb was performed as follows. Under general anesthesia, the hind limb of a 3-month-old mouse was tightened right beneath the inguinal ligament with a rubber band to isolate the blood stream from the systemic circulation. Because of the difficulty of catheter insertion into the femoral artery, retrograde perfusion via the femoral vein was performed. One half of a milliliter of viral solution or saline were slowly injected (over 3 min) into the femoral vein. The blocked blood stream of the lower limb was reopened 20 min after perfusion.

**Detection of transgene expression.** To examine the whole body expression of the enhanced green fluorescent protein, GFP (Clontech), we killed the mice or hamsters and removed skin and subcutaneous fat tissue. A handheld, long-wavelength UV lamp (Multiband UV –254/366nm, Model UVGL-58, UVP Inc.) was used to illuminate the mice. Whole-body photographs were taken with a Nikon E5700 digital camera. We then prepared 6-µm cryosections of various tissues for microscopic examination. GFP expressions were observed using a Nikon TE-300 fluorescent microscope with Spot digital camera. For quantitative analysis of the intensity levels of GFP expression, 12-bit monochrome photographs (4× objective lens) were taken, and the exposure conditions were maintained throughout the experiments to keep the data comparable. The average intensities were analyzed by the MetaMorph software (Meta Imaging Series, version 6.1) from Universal Imaging Corporation and the average grade level was used as the unit of fluorescence intensity in tissues. The intensity of GFP expression was presented as the obtained intensity minus the background intensity of corresponding tissues from mice without AAV vector treatment. Immunofluorescent staining of sarcoglycan was performed as described previously<sup>33</sup>.

Note: Supplementary information is available on the Nature Biotechnology website.

#### ACKNOWLEDGMENTS

We thank Michelle Raab for critical reading of the manuscript; Guangping Gao and James Wilson for the AAV7 and 8 packaging plasmid; David W. Russell for the AAV6 packaging plasmid. This work is supported by National Institutes of Health grants NS46546, AR45967 and AR50595 to X.X.

#### COMPETING INTERESTS STATEMENT

The authors declare that they have no competing financial interests.

Received 8 November 2004; accepted 24 January 2005

Published online at <http://www.nature.com/naturebiotechnology/>

1. Watchko, J. *et al.* Adeno-associated virus vector-mediated minidystrophin gene therapy improves dystrophic muscle contractile function in mdx mice. *Hum. Gene Ther.* **13**, 1451–1460 (2002).

2. Wang, B., Li, J. & Xiao, X. From the cover: adeno-associated virus vector carrying human minidystrophin genes effectively ameliorates muscular dystrophy in mdx mouse model. *Proc. Natl. Acad. Sci. USA* **97**, 13714–13719 (2000).
3. van Deutekom, J.C. & van Ommen, G.J. Advances in Duchenne muscular dystrophy gene therapy. *Nat. Rev. Genet.* **4**, 774–783 (2003).
4. Harper, S.Q. *et al.* Modular flexibility of dystrophin: implications for gene therapy of Duchenne muscular dystrophy. *Nat. Med.* (see comments) **8**, 253–261 (2002).
5. Manno, C.S. *et al.* AAV-mediated factor IX gene transfer to skeletal muscle in patients with severe hemophilia B. *Blood* **101**, 2963–2972 (2003).
6. Song, S. *et al.* Sustained secretion of human alpha-1-antitrypsin from murine muscle transduced with adeno-associated virus vectors. *Proc. Natl. Acad. Sci. USA* **95**, 14384–14388 (1998).
7. Fraites, T.J. Jr. *et al.* Correction of the enzymatic and functional deficits in a model of pompe disease using adeno-associated virus vectors. *Mol. Ther.* **5**, 571–578 (2002).
8. Xiao, X., Li, J. & Samulski, R.J. Efficient long-term gene transfer into muscle tissue of immunocompetent mice by adeno-associated virus vector. *J. Virol.* **70**, 8098–8108 (1996).
9. Kessler, P.D. *et al.* Gene delivery to skeletal muscle results in sustained expression and systemic delivery of a therapeutic protein. *Proc. Natl. Acad. Sci. USA* **93**, 14082–14087 (1996).
10. Fisher, K.J. *et al.* Recombinant adeno-associated virus for muscle directed gene therapy. *Nat. Med.* **3**, 306–312 (1997).
11. Kawada, T. *et al.* Rescue of hereditary form of dilated cardiomyopathy by rAAV-mediated somatic gene therapy: amelioration of morphological findings, sarcolemmal permeability, cardiac performances, and the prognosis of TO-2 hamsters. *Proc. Natl. Acad. Sci. USA* **99**, 901–906 (2002).
12. Budker, V., Zhang, G., Danko, I., Williams, P. & Wolff, J. The efficient expression of intravascularly delivered DNA in rat muscle. *Gene Ther.* **5**, 272–276 (1998).
13. Greelish, J.P. *et al.* Stable restoration of the sarcoglycan complex in dystrophic muscle perfused with histamine and a recombinant adeno-associated viral vector. *Nat. Med.* **5**, 439–443 (1999).
14. Hoshijima, M. *et al.* Chronic suppression of heart-failure progression by a pseudophosphorylated mutant of phospholamban via in vivo cardiac rAAV gene delivery. *Nat. Med.* **8**, 864–871 (2002).
15. Li, J. *et al.* Efficient and long-term intracardiac gene transfer in delta-sarcoglycan-deficiency hamster by adeno-associated virus-2 vectors. *Gene Ther.* **10**, 1807–1813 (2003).
16. Rucker, M. *et al.* Rescue of enzyme deficiency in embryonic diaphragm in a mouse model of metabolic myopathy: pompe disease. *Development* **131**, 3007–3019 (2004).
17. Cordier, L. *et al.* Rescue of skeletal muscles of gamma-sarcoglycan-deficient mice with adeno-associated virus-mediated gene transfer. *Mol. Ther.* **1**, 119–129 (2000).
18. Dressman, D. *et al.* Delivery of alpha- and beta-sarcoglycan by recombinant adeno-associated virus: efficient rescue of muscle, but differential toxicity. *Hum. Gene Ther.* **13**, 1631–1646 (2002).
19. Chao, H. *et al.* Several log increase in therapeutic transgene delivery by distinct adeno-associated viral serotype vectors. *Mol. Ther.* **2**, 619–623 (2000).
20. Hammermann, M. *et al.* Salt-dependent DNA superhelix diameter studied by small angle neutron scattering measurements and Monte Carlo simulations. *Biophys. J.* **75**, 3057–3063 (1998).
21. Yoshida, K. *et al.* Fabrication of a new substrate for atomic force microscopic observation of DNA molecules from an ultrasmooth sapphire plate. *Biophys. J.* **74**, 1654–1657 (1998).
22. Pruchnic, R. *et al.* The use of adeno-associated virus to circumvent the maturation-dependent viral transduction of muscle fibers. *Hum. Gene Ther.* **11**, 521–536 (2000).
23. Xiao, W. *et al.* Gene therapy vectors based on adeno-associated virus type 1. *J. Virol.* **73**, 3994–4003 (1999).
24. Gao, G.P. *et al.* Novel adeno-associated viruses from rhesus monkeys as vectors for human gene therapy. *Proc. Natl. Acad. Sci. USA* **99**, 11854–11859 (2002).
25. Gao, G. *et al.* Clades of adeno-associated viruses are widely disseminated in human tissues. *J. Virol.* **78**, 6381–6388 (2004).
26. Summerford, C. & Samulski, R.J. Membrane-associated heparan sulfate proteoglycan is a receptor for adeno-associated virus type 2 virions. *J. Virol.* **72**, 1438–1445 (1998).
27. Walters, R.W. *et al.* Binding of adeno-associated virus type 5 to 2,3-linked sialic acid is required for gene transfer. *J. Biol. Chem.* **276**, 20610–20616 (2001).
28. Di Pasquale, G. *et al.* Identification of PDGFR as a receptor for AAV-5 transduction. *Nat. Med.* **9**, 1306–1312 (2003).
29. Kaludov, N., Brown, K.E., Walters, R.W., Zabner, J. & Chiorini, J.A. Adeno-associated virus serotype 4 (AAV4) and AAV5 both require sialic acid binding for hemagglutination and efficient transduction but differ in sialic acid linkage specificity. *J. Virol.* **75**, 6884–6893 (2001).
30. Wang, Z. *et al.* Rapid and highly efficient transduction by double-stranded adeno-associated virus vectors in vitro and in vivo. *Gene Ther.* **10**, 2105–2111 (2003).
31. Xu, L. *et al.* CMV-beta-actin promoter directs higher expression from an adeno-associated viral vector in the liver than the cytomegalovirus or elongation factor 1 alpha promoter and results in therapeutic levels of human factor X in mice. *Hum. Gene Ther.* **12**, 563–573 (2001).
32. Gregorevic, P. *et al.* Systemic delivery of genes to striated muscles using adeno-associated viral vectors. *Nat. Med.* **10**, 828–834 (2004).

33. Li, J. *et al.* rAAV vector-mediated sarcoglycan gene transfer in a hamster model for limb girdle muscular dystrophy. *Gene Ther.* **6**, 74–82 (1999).
34. Li, X., Eastman, E.M., Schwartz, R.J. & Draghia-Akli, R. Synthetic muscle promoters: activities exceeding naturally occurring regulatory sequences. *Nat. Biotechnol.* **17**, 241–245 (1999).
35. Hagstrom, J.E. *et al.* A facile nonviral method for delivering genes and sirnas to skeletal muscle of mammalian limbs. *Mol. Ther.* **10**, 386–398 (2004).
36. Arruda, V.R. *et al.* Regional intravascular delivery of AAV-2-F.IX to skeletal muscle achieves long-term correction of hemophilia B in a large animal model. *Blood*; published online 12 October 2004.
37. Lee, C.G. *et al.* Vascular endothelial growth factor (VEGF) induces remodeling and enhances T(H)2-mediated sensitization and inflammation in the lung. *Nat. Med.* **10**, 1095–1103 (2004).
38. Kern, A. *et al.* Identification of a heparin-binding motif on adeno-associated virus type 2 capsids. *J. Virol.* **77**, 11072–11081 (2003).
39. Hauck, B., Chen, L. & Xiao, W. Generation and characterization of chimeric recombinant AAV vectors. *Mol. Ther.* **7**, 419–425 (2003).
40. Rabinowitz, J.E. *et al.* Cross-dressing the virion: the transcapsidation of adeno-associated virus serotypes functionally defines subgroups. *J. Virol.* **78**, 4421–4432 (2004).
41. Shi, W., Arnold, G.S. & Bartlett, J.S. Insertional mutagenesis of the adeno-associated virus type 2 (AAV2) capsid gene and generation of AAV2 vectors targeted to alternative cell-surface receptors. *Hum. Gene Ther.* **12**, 1697–1711 (2001).
42. Loiler, S.A. *et al.* Targeting recombinant adeno-associated virus vectors to enhance gene transfer to pancreatic islets and liver. *Gene Ther.* **10**, 1551–1558 (2003).
43. Bartlett, J.S., Kleinschmidt, J., Boucher, R.C. & Samulski, R.J. Targeted adeno-associated virus vector transduction of nonpermissive cells mediated by a bispecific F(ab'gamma)2 antibody. *Nat. Biotechnol.* (erratum in *Nat. Biotechnol.* **17**, 393, 1999) **17**, 181–186 (1999).
44. Xiao, X., Li, J. & Samulski, R.J. Production of high-titer recombinant adeno-associated virus vectors in the absence of helper adenovirus. *J. Virol.* **72**, 2224–2232 (1998).
45. Rabinowitz, J.E. *et al.* Cross-packaging of a single adeno-associated virus (AAV) type 2 vector genome into multiple AAV serotypes enables transduction with broad specificity. *J. Virol.* **76**, 791–801 (2002).
46. Rutledge, E.A., Halbert, C.L. & Russell, D.W. Infectious clones and vectors derived from adeno-associated virus (AAV) serotypes other than AAV type 2. *J. Virol.* **72**, 309–319 (1998).
47. Li, J., Samulski, R.J. & Xiao, X. Role for highly regulated rep gene expression in adeno-associated virus vector production. *J. Virol.* **71**, 5236–5243 (1997).
48. Snyder, R., Xiao, X. & Samulski, R.J. Production of recombinant adeno-associated viral vectors. in *Current Protocols in Human Genetics* (eds. Dracopoli, N. *et al.*) 12.11.11–12.12.23 (John Wiley & Sons Ltd., New York, 1996).
49. Sands, M.S. & Barker, J.E. Percutaneous intravenous injection in neonatal mice. *Lab. Anim. Sci.* **49**, 328–330 (1999).